Instantaneous PLII and OH chemiluminescence study on wide distillation fuels, PODEn and ethanol blends in a constant volume vessel

Cui, Longxi; Ma, Yue; Liu, Dong; Ma, Xiao; Xu, Hongming; Shuai, Shijin

DOI:
10.4271/2020-01-0340

20XX-01-XXXX

Instantaneous PLII and OH* Chemiluminescence Study on Wide Distillation Fuels, $PODE_n$ and Ethanol Blends in a Constant Volume Vessel

Author, co-author (Do NOT enter this information. It will be pulled from participant tab in MyTechZone)
Affiliation (Do NOT enter this information. It will be pulled from participant tab in MyTechZone)

Abstract

The combustion characteristics and soot emissions of three types of fuels were studied in a high pressure and temperature vessel. In order to achieve better volatility, proper cetane number and high oxygen content, the newly designed WDEP fuel was proposed and investigated. It is composed of wide distillation fuel (WD), $PODE_{3-6}$ mixture ($PODE_n$) and ethanol. For comparison, the test on WD and the mixture of $PODE_n$-ethanol (EP) are also conducted. OH* chemiluminescence during the combustion was measured and instantaneous PLII was also applied to reveal the soot distribution. Abel transformation was adopted to calculate the total soot of axisymmetric flame. The results show that WDEP has similar ignition delays and flame lift-off lengths to those of WD at 870-920 K. But the initial ignition locations of WDEP flame in different cycles were more concentrated, particularly under the condition of low oxygen atmosphere. Comparing with WD, the soot amount of WDEP decreased for 55% and 27% at 870 K and 920 K. For the case of 920 K and 15.8% of ambient oxygen, the soot amount in WDEP case decreased by 44%, indicating a more significant soot reduction effect at lower temperatures and EGR conditions.

Introduction

With the increasingly strict emission regulations, more and more attention has been paid to the problem of high NOx and PM emissions of traditional compression ignition (CI) engines. In this regard, one of the strategies is to adopt the combustion mode of partial premixed compression ignition (PPCI) [1,2], that is, to form a premixed charge before combustion to reduce the proportion of diffusion combustion. This puts forward new requirements for the fuel. The fuel suitable for PPCI should have better volatility and lower cetane number than commercial diesel to form a better premix before ignition [3]. Wide distillation fuel (WD) [4], namely a kind of hydrocarbon fuel with distillation range from the initial distillation point of gasoline to the final distillation point of diesel, possess the characteristics above. In the long term, a kind of long distillation range fuel which can be obtained from petroleum by single distillation has the potential to simplify the refining process and reduce the refining cost. Furthermore, the demand for heavier fuels such as diesel will rise more significantly than gasoline in the future [5]. Changing the demand of traditional diesel fuel to that of WD can help to deal with the demand structure problem.

A large number of PPCI research using WD [6-10] have been reported. However, in conditions with high load and low speed, PPCI combustion often presents concentrated single-stage heat release, resulting in high maximum pressure rise rate (MPRR) and high NOx emissions. It limits the load expansion of wide distillation fuel in PPCI combustion mode. Yang et al. proposed a new combustion mode called multiple premixed compression ignition (MPCI), which is one of the ways to reduce MPRR and shows more potential in emission control [11]. In this mode, spray and combustion events are organized as "spray-combustion-spray-combustion" mode, and the two premixed combustion events are designed to be separated both in time and space. Actual engine experiments have been conducted to reveal the feasibility of MPCI fueled with naphtha and dieseline [12, 13], and the MPCI combustion mode achieved lower MPRR than PPCI. However, at high engine speed and heavy load, the proportion of diffusion combustion increased and the soot emission increased due to the over-short mixing time and high ambient temperature of the second combustion event, especially for low RON fuels.

Polyoxymethylene Dimethyl Ethers ($PODE_n$), a kind of diesel alternative fuel with high ignitability and nearly 50% oxygen content, has been proved to be effective in reducing the formation of soot in diffusion flame [14-16]. Its physical and chemical properties are shown in Table 1. Liu et al. added 20% $PODE_n$ to WD and tested its performance in PPCI mode [17]. The results showed that compared with WD, the blended fuel significantly reduced the soot emission, but had shorter ignition delay and combustion duration, resulting in slightly higher NOx emission. It is not difficult to find that $PODE_n$ is suitable for reducing soot emission in MPCI, but the over high cetane number (>70) of $PODE_n$ changes the ignitability of WD. Therefore, it is necessary to add a kind of fuel with high RON into PODEn, making the ignitability of the blended fuel similar to that of WD.

Ethanol has low boiling point (78.5 °C), high oxygen content and high RON (108). Thus the blends of ethanol and $PODE_n$ (EP) will have lower cetane number than $PODE_n$ while maintaining the high oxygen content and good volatility. Finally, by mixing EP fuel in WD, a WDEP fuel can be obtained. The ignitability of fuel is considered, which makes the properties of WDEP fuel might be more suitable for PPCI and MPCI mode. As WD fuel from different sources may have different ignition properties, it is necessary to consider adjusting its ignitability. By mixing WD with different proportions of ethanol and $PODE_n$, WDEP fuel can reach the appropriate ignitability. This type of blend fuel also has advantages in environmental sustainability because $PODE_n$ and ethanol can be produced from renewable feedstocks, like biomass. To the best of the authors' knowledge, such fuel design scheme has not been reported before.

In this study, the ignitability and soot formation characteristics of WD and WDEP were investigated in a constant-volume vessel. Ignition delay, flame lift-off length (LOL) and the distribution of ignition points were analyzed by high speed OH* chemiluminescence, soot

amount and distribution in steady and transient states were obtained by quasi-steady PLII and time-varying PLII. Abel transformation was adopted to calculate soot amount in 3-D space.

Experimental Setup

The physical and chemical properties of the fuels used in this study are listed in Table 1. Wide distillation fuel was provided by local supplier of China, with the T10 of 99.8 °C, the T50 of 182.4 °C and the T90 of 314.6 °C. The $PODE_n$ used are samples from mass production, containing 48.8% of $PODE_3$, 27.3% of $PODE_4$, 13.7% of $PODE_5$ and 7.7% of $PODE_6$ by mass fraction.

In this study, after pre-experiment, the following fuel ratio is determined: The volume ratio of ethanol to $PODE_n$ in EP is 3:7. The volume ratio of EP in WDEP is 20%.

Table 1. Physical and chemical properties of the fuels used.

Fuel	WD	Ethanol	$PODE_n$
Distillation range (°C)	99.8-314.6	78.5	156-280
Density (g/cm^3)	0.863	0.789	1.019
RON	-	108	-
CN	32.5	-	78.4
O (%(m/m))	-	34.78%	47.11%

Table 2 shows the ambient and injection conditions of this work. Considering the good evaporation of wide distillation fuel, an injection pressure of 60 MPa is high enough. The 4 MPa ambient pressure and 820-920 K ambient temperature were chosen to represent the cylinder conditions when fuel is injected the second time in MPCI mode. The ambient oxygen concentration of 21% and 15.8% (others are nitrogen) roughly correspond to EGR rate of 0% and 25%. In OH* chemiluminescence and quasi-steady PLII tests, the injection duration was 5.0 ms to achieve quasi-steady combustion stage, while in time-varying PLII test, the injection duration was 1.0 ms, which is convenient to study the whole combustion process.

Table 2. Summary of test conditions.

Ambient pressure	4 MPa
Ambient temperature	820 K, 870 K, 920 K
Ambient oxygen concentration	21%, 15.8%
Injection pressure	60 MPa
Injection duration	1 ms, 5 ms

The experiments are based on a high-temperature and high-pressure constant volume combustion vessel as shown in Figure 1. Four quartz windows with a diameter of 100 mm are evenly distributed on four sides as optical accesses. The volume of the chamber is 0.017 m^3 and the heating cartridges are installed at the bottom. A single-hole injector (d=0.168 mm) was mounted at the top of the chamber. Complete information about the constant volume vessel and the control of the ambient conditions can be found in our previous papers [18].

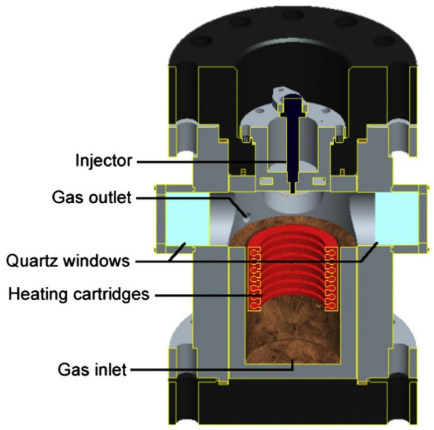

Figure 1. Section diagram of the constant volume vessel [18].

Figure 2 shows the schematic figure of the optical set-up for the OH* chemiluminescence imaging and PLII test. For the OH* chemiluminescence imaging, a high-speed image intensifier (Lavision HS-IRO) was coupled with a high-speed camera (Photron FASTCAM SA-Z). And then was equipped with a 100-mm UV lens and a 308 nm band-pass filter (FWHM 8 nm). The aperture was fixed as F/2.8. The OH* chemiluminescence images were obtained during the entire process of combustion. The frame rate was 20000 frames per second and the resolution was 640 x 1024 pixels. High-speed camera was triggered at the same time as the start of injector energizing. Gain duration of the intensifier was 18 μs per shot and it was completely included in the exposure time of high-speed camera. At each test point, OH* chemiluminescence imaging was repeated for 20 cycles.

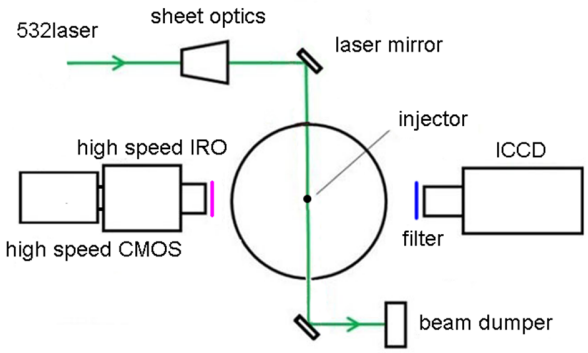

Figure 2. Sketch of the optical setup.

For the LII test, a Nd:YAG laser device (Quantel Brilliant B) was used and the laser frequency was doubled thus the output laser was 532 nm. The laser beam (310 mJ per pulse, 10 Hz) was converted into a 80-mm wide, 0.6-mm thick laser sheet by the sheet optics. The laser sheet was located on the axis of the injector. The spatial average laser fluence was about 0.3 J/cm^2 considering the energy lose in the sheet optics and the quartz window, above the threshold of about 0.2 J/cm^2 for 532 nm laser excitation [19], hence the LII signal was nearly independent of laser fluence variations. In this research, laser attenuation was not significant in most parts of the soot area, but in some specific areas, laser attenuation was strong enough that the local energy in the laser exit side may fall out of the “plateau region”. The similar phenomena have been discussed by Pickett et al. [20] and the authors’ previous

research [18]. So only the LII signal of inlet side (divided by the spray axis) was used as valid data to ensure the reliability.

An (Princeton Instrument PM4) ICCD camera was used to get the PLII image, which was equipped with a 90 mm lens and a 410 nm band-pass filter (FWHM 50 nm), and the aperture was fixed as F/2.8. In the quasi-steady PLII test, the spray duration was 5 ms and the laser was shot 4.5 ms after the energizing of the injector. In the time-varying PLII test, the spray duration was 1 ms and the laser was shot from 1.8 ms to 4.4 ms after the energizing of the injector, the interval between two adjacent test points was 0.2 ms. The ICCD gate was opened 10 ns after the laser shot and lasts for 30 ns. Gain of the ICCD was fixed. Each PLII test point was repeated for 20 times and ensemble-averaged.

Results and Discussion

OH Chemiluminescence Test*

In this study, the time when the maximum connected component area of OH* signal first exceeds 40 pixels (corresponding to about 1/3 mm^2 of the flame kernel) is marked as the start of ignition. The ignition delay is defined as the time interval from the start of injection signal pulse (SOP) to the start of ignition. The initial ignition position is defined as the barycentric coordinates of the foresaid maximum connected component. The flame gets relatively stable in 4-6 ms after the SOP, so the 40 pictures in this period were time-averaged. The flame lift-off length (LOL) is defined as the initial location where the signal intensity exceeds a threshold. The threshold is chosen as 50% of the value at the end of the rapid rise stage of the signal, as defined by Siebers [21] et al.

Ignition Delay

Figure 3 shows the ignition delay of tested fuels in different ambient oxygen concentration and temperature. Error bars show one standard deviation. The cases with 15.8% ambient oxygen concentration are marked as 'EGR'. At high temperature (870 K and 920 K) cases, the ignition delay of WDEP and WD are similar. At 820 K, WDEP has a longer ignition delay, while at 920 K and low oxygen atmosphere, WDEP has a shorter ignition delay. The start of ignition is affected by the heat transfer from the ambient air, the accumulated energy in the low-temperature reaction and the heat absorption of fuel evaporation. At lower ambient temperature, the heat transfer from ambient air is low. For WDEP fuel, the enthalpy of vaporization of ethanol is larger, so the temperature at the same location is lower, and thus the ignition delay is longer. When the temperature is higher, the heat transfers from the air increases and the influence of evaporation enthalpy decreases. At this condition, the ignition delay of WD and WDEP tends to be similar. At low oxygen atmosphere cases, the low-temperature heat release of both fuels is inhibited. The oxygen content of WDEP is higher, which means it is easier to reach the air-fuel ratio that suitable for ignition, so its low-temperature heat release is faster than WD, results in a shorter ignition delay.

On the whole, from 820 K to 870 K, the decrease of ignition delay is more significant for WDEP than WD, while from 870 K to 920 K, the ignition delay of WD and WDEP is similar. The ignition delay of WDEP is less sensitive to ambient oxygen concentration than that of WD.

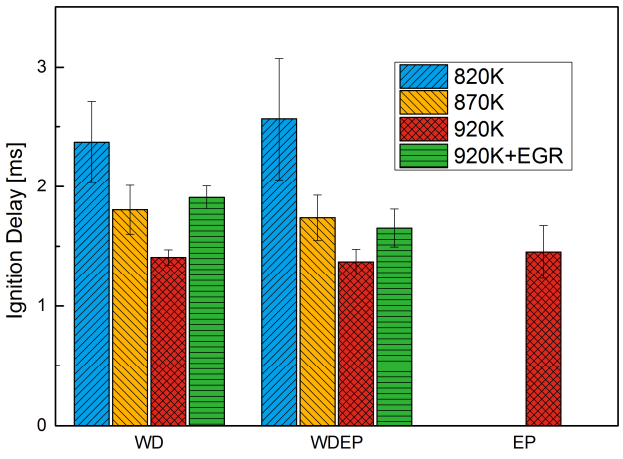

Figure 3. Ignition delay of tested fuels in different ambient conditions.

Flame Lift-off Length and OH* Initial Position Distribution

Figure 4 shows the ensemble-averaged OH* chemiluminescence images of tested fuels in different ambient oxygen concentration and temperature. The location of the injector tip is marked in the figure by red triangles. In WD and WDEP cases, a part of the strong signal in the downstream region (y axis > 40 mm) is the UV band radiation of high temperature soot according to Siebers' previous research [21]. While in the upstream areas, the OH* signal dominates. In the upstream areas, the OH* signal of WD and WDEP fuels distributed in the outer region of flame, especially in low ambient oxygen concentration cases. This is because the over-rich mixture in the central region inhibited the oxidation. Hence the temperature was low and formation of OH* was weak. The case of the EP fuel was completely opposite, the OH* chemiluminescence was aggregated in the central region and was much stronger than WD or WDEP fuel cases. In addition to the influence of local air-fuel ratio, more OH* was produced in the oxidation process of EP. The better volatility of EP fuel led to a large proportion of premixed combustion and resulted in more concentrated OH* production.

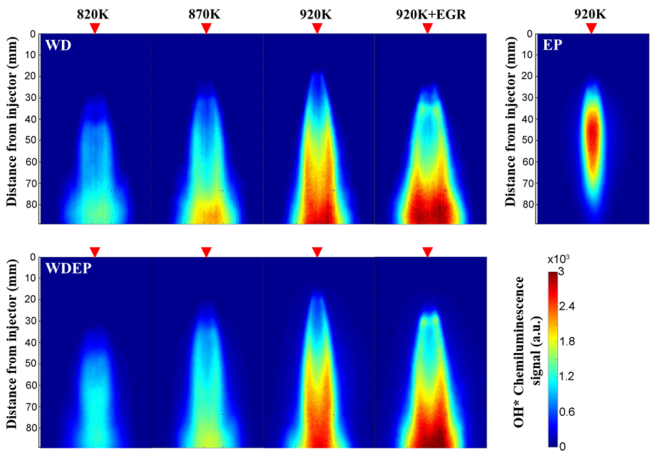

Figure 4. Ensemble-averaged OH* chemiluminescence images of tested fuels.

Figure 5 shows the average LOL. The LOL of WD and WDEP was almost the same in cases of 870 K and 920 K with 21% ambient oxygen concentration. In lower temperature of 820 K, the LOL of WDEP was much longer than that of WD and the cyclic fluctuation was more significant. This phenomenon can be explained by the model reported by Persson et al. [22]. The LOL was affected by temperature downstream the lift-off position and fuel ignitability. Because of the lower heating value and relatively high latent heat of evaporation of $PODE_n$ and ethanol, the flame temperature downstream the lift-off position of WDEP will be lower than that of WD, resulting in longer LOL. In the cases of lower ambient temperature, the aforementioned phenomenon will become more significant. Because of the same reason, even at 920 K, the LOL of EP was still significantly longer than that of WD based fuels. At low oxygen atmosphere cases, LOL of WDEP was slightly shorter than that of WD, which reflects the influence of local air-fuel ratio. Under similar air entrainment conditions, WDEP fuel was easier to achieve the appropriate fuel-air equivalence ratio in EGR cases because of its lower stoichiometric ratio. This shows that WDEP fuel has better tolerance to high EGR conditions, which is beneficial to match the second combustion of MPCI mode as mentioned before.

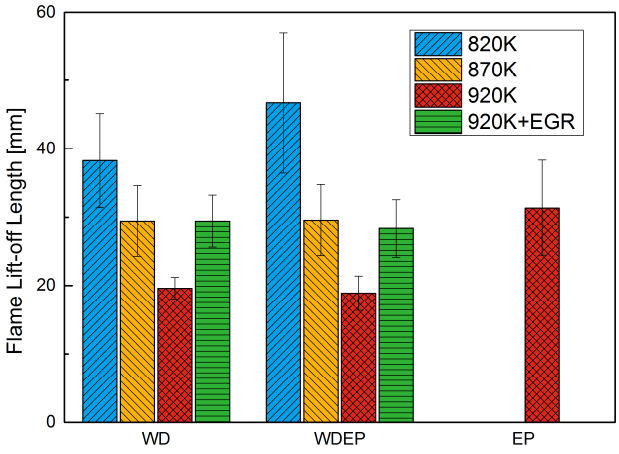

Figure 5. Flame lift-off length of the investigated fuels in different ambient conditions.

The height of initial ignition position is shown in Figure 6. It is shown that the initial ignition position of WD and WDEP is similar at high oxygen atmosphere cases even when the temperature was low. The influence of temperature on the initial ignition position of different fuels is less than that on LOL. In the typical process of diffusion flame, the flame first occurs at a downstream location and then travels upstream until it stabilizes at the lift-off position [23]. In the 820 K cases, the flame upper edge of WD traveled by 20.4 mm from the initial ignition position to the lift-off position, while for WDEP, the distance was only 13.2 mm. Different from the LOL, which is affected by the heat release of the downstream high-temperature combustion, the initial ignition position is mainly affected by the accumulated energy of the low-temperature reaction. As a fuel with high cetane number and high oxygen content, the $PODE_n$ components in WDEP result in a lower heat release in high-temperature combustion stage but a higher heat release in the low-temperature combustion stage, thus causing different temperature sensitivities in LOL and initial ignition position height.

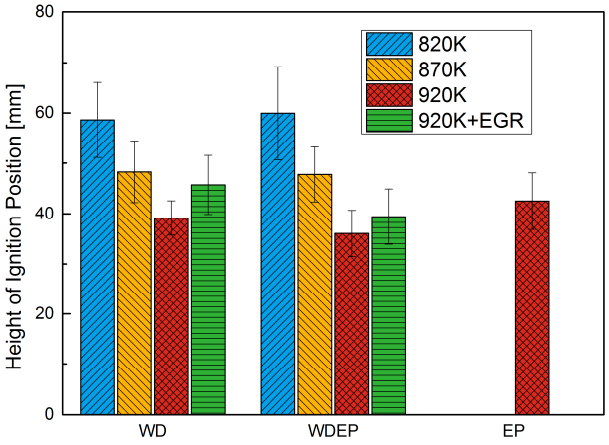

Figure 6. Height of ignition position of the investigated fuels in different ambient conditions.

Another problem worthy of discussing is the horizontal distribution of initial ignition point. Assuming that the flame is centrosymmetric, variance of the abscissa of every initial ignition points was calculated as shown in Figure 7. A smaller variance indicates that the ignition points are more concentrated in transverse distribution. The OH* signal is accumulated along the optical path (the direction of camera axis), which means that the initial ignition positions close to the axis in the images are not necessarily close to the axis in fact, but the initial ignition positions far away from the axis in the images must be far away from the axis of the nozzle. Therefore, the dispersion degree of the initial ignition position of the OH* image accumulated along the optical path can still reflect the dispersion degree of the actual initial ignition position. Figure 7 shows that the variance first increases and then decreases with the increase of temperature. At a low ambient temperature of 820 K, the ignition height is long. At this height, the region where the local air fuel ratio suitable for ignition is distributed near the axis, which is more conducive to the emergence of the ignition point. When the environment temperature increases to 870 K, the ignition height decreases, and the region with suitable air-fuel ratio is distributed farther from the axis. So at 870 K, the transverse distribution of initial ignition point is more scattered. As the temperature rises further to 920 K, the ignition point moves upward, and the initial ignition points can only appear in a more concentrated area due to the conical structure of the spray. Under conditions with low oxygen atmosphere, the ignition point distribution of WDEP fuel is more concentrated than that of WD. As analyzed before, this is mainly because the region with appropriate fuel air equivalence ratio is closer to the axis for WDEP. In general, the transverse distribution of ignition point of WDEP fuel is more concentrated than that of WD fuel.

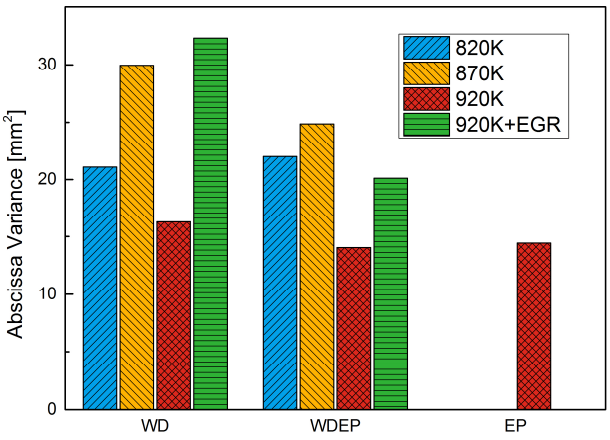

Figure 7. Variance of the abscissa of each initial ignition points of tested fuels in different ambient conditions.

PLII Test

Quasi-Steady Flame PLII

Figure 8 reveals the ensemble-averaged soot distribution on the half cross-section of WD and WDEP fuels in different ambient temperature and oxygen concentration. The flame axis is on the left edge of each image. The scale plate on the left side of the images marks the vertical distance from the injector tip. The ambient conditions are marked in the image. At 820 K, the LII signal value of WDEP fuel was very weak, so it's not shown in the figures. The LII signal of EP was very weak at every ambient condition tested, so the LII test of EP fuel will not be discussed in this study. Figure 9 shows the accumulated LII signal (pixel grayscale) value on the tested half cross-section. The values were normalized based on that of WD at 920 K. Assuming that the flame was axisymmetric, the total amount of soot in 3-D space can be calculated from the signal value of the test plane by Abel transformation, as shown in Figure 10, also normalized.

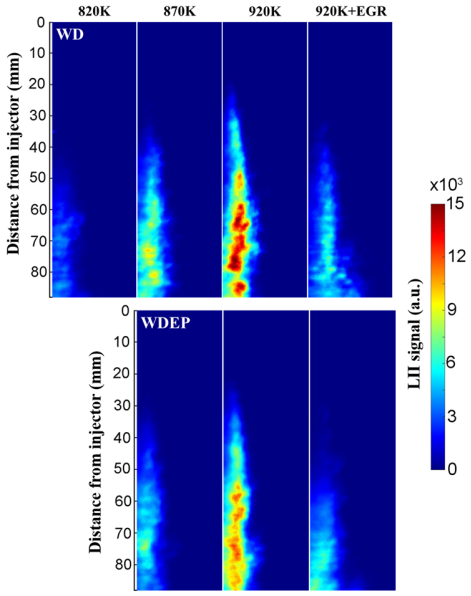

Figure 8. Soot distribution of WD and WDEP in different ambient conditions.

The addition of 20% EP fuel significantly reduced the soot concentration in WD quasi-steady state flames. At 870 K and 920 K, the amount of soot decreased by 55% and 27%, while at 920 K with EGR, it decreased by 44%. The formation of soot in diffusion flame mainly depends on the local temperature and the air-fuel ratio. As WDEP just containing a low percentage of EP, it can be predicted that the spray characteristics of WD and WDEP fuel are similar. Therefore, air entrainment downstream the lift-off position is also similar. The overall equivalence ratio was lower for WDEP fuels because of its lower stoichiometric air-fuel ratio. And the absence of C-C bond in the molecule of $PODE_n$ also reduced the generation of soot precursors.

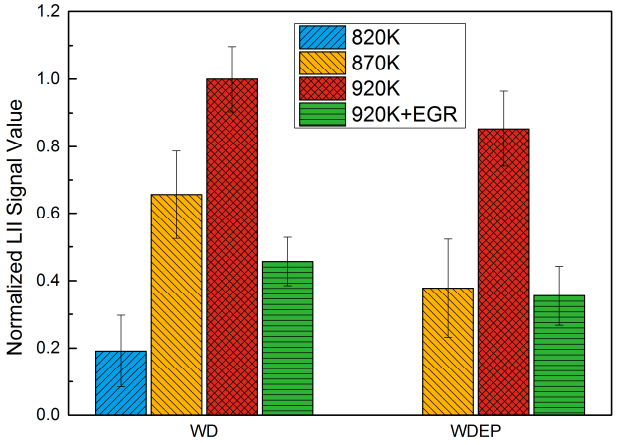

Figure 9. Accumulated LII signal value on the test cross-section.

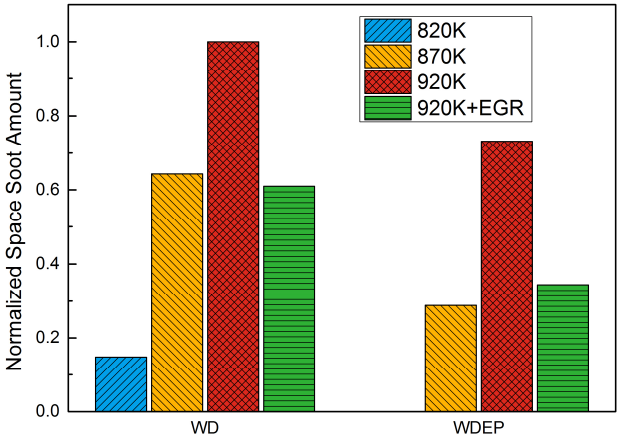

Figure 10. Space total soot amount in the tested region.

Comparing Figure 9 with Figure 10, it is found that in different cases, there are some differences between the soot intensity on the test plane and in the 3-D space. This is because of the differences in the spatial distribution of soot. The rich soot area which is farther away from the axis of the injector results in higher spatial soot accumulation after Abel transformation. For example, the plane LII signal of low oxygen atmosphere condition is significantly lower than that of high oxygen atmosphere condition. However, their difference is narrowed after the Abel transformation. This indicates that the rich soot area locates farther from the axis in the low oxygen atmosphere case.

The soot distribution characteristics along the radial direction were shown in Figure 11. The LII signal value of the pixels in the same

distance from flame axis were added up and plotted along the distance from the flame axis. The addition of EP made the thick soot area shifts to the center of the flame at all cases. In the center area, the local equivalence ratio was decreased, and reaction was promoted and the temperature got higher. The local high temperature and lack of oxygen required for soot generation are met at the same time. In the outer area of the flame, the mixture of WDEP fuels were leaner than that of WD, resulting in less soot formation and faster oxidation. So the soot area is "thinner" with the increase of in-fuel oxygen content. For the same reason, at low oxygen atmosphere conditions, soot distribution got more dispersed and the soot area got wider.

At low temperature and low oxygen atmosphere conditions, the soot reduction effect of WDEP fuel was more significant. This can also be explained by the distribution of soot. For WD, with the decrease of ambient temperature, the distribution area of soot only slightly shifts in, but for WDEP, the shift-in was quiet notable. This is due to the lower heat value of WDEP, when the ambient temperature is lower, its flame high-temperature region move faster toward the center of the flame. At low oxygen atmosphere, soot distribution got more dispersed, however, WDEP fuel partly resisted this trend due to its high in-fuel oxygen content. Therefore, WDEP fuel is easier to achieve a smaller soot distribution area at low temperature and low oxygen atmosphere, finally reduces the total soot amount.

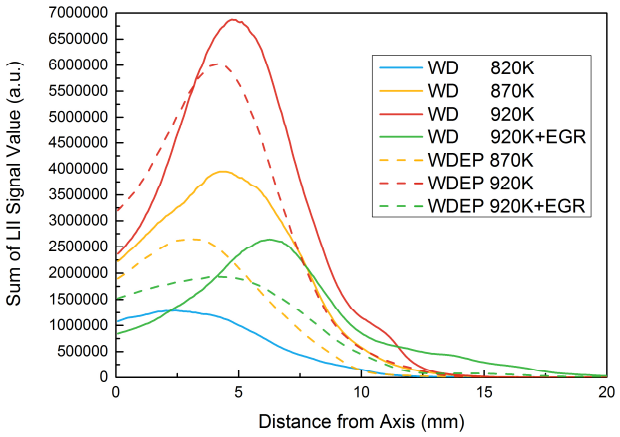

Figure 11. The sum of soot signal value of all the pixels in the same distance from flame axis.

Figure 12 shows distribution characteristics along the axial direction. The LII value of the pixels with the same ordinate was added up and plotted along the vertical distance from injector. Considering the correlation between the vertical distance from injector and the fuel injection process, this image can reflect the time-varying characteristics of soot. At high oxygen atmosphere conditions, the soot signal rises first, reaches the peak value and then decreases, this reflects the formation-oxidation process of soot. However, in the cases of low oxygen atmosphere conditions, the oxidation of soot is weak, and soot signal value has been on the rise in the whole tested range. With the addition of oxygenated fuel, the rate of soot formation slows down significantly at lower temperature and low oxygen atmosphere conditions due to the relatively thin soot formation region. At 920 K, the soot production of WDEP and WD were similar in the early stage, but the peak value of soot of WDEP was lower.

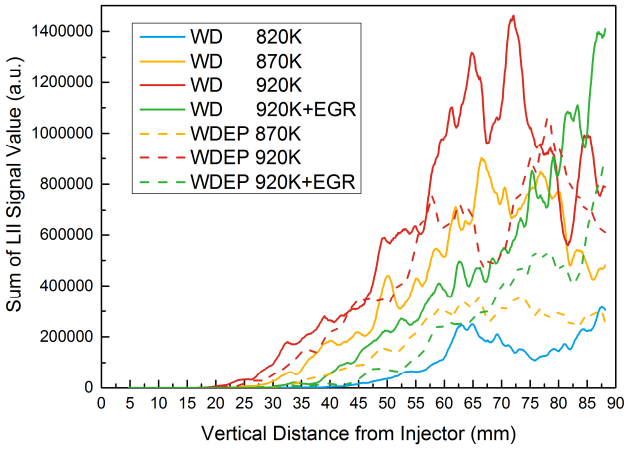

Figure 12. The sum of soot signal value of all the pixels in the same vertical distance from the height of injector tip.

Time-varying PLII

The time-varying images of soot distribution under different ambient temperature and oxygen concentration are shown in Figure 13. The images are ensemble averaged. The flame axis is on the left edge of each image. The variation of space total amount of soot with time after injection is shown in Figure 14.

As shown in Fig 13a and 14a, at low temperature, the soot amount of WDEP fuel was significantly less than that of WD. Soot was produced later and less, the peak value reached earlier, which means the soot oxidation rate exceeds the soot generation rate earlier. When the ambient temperature got higher, as shown in Figure 13b and 14b, the effect of WDEP on reducing soot formation was weakened. The formation of soot is almost the same in the early stage of the two fuels, which is consistent with the phenomenon shown in Figure 12. One possible explanation is that soot formation is related to the mixing of fuel and air. WDEP has better evaporation than WD, so its soot formation rate is lower. When the ambient temperature is low, this advantage is significant, while when the ambient temperature is higher, the evaporation rate of WD is promoted as well, and the difference between WD and WDEP is smaller.

Figure 14b shows that the main reason for the low soot peak value of WDEP is that its soot distribution area is relatively thin and basically distributed near the flame axis. For WD fuel, some soot moved to the outer edge of the flame, especially in the later stage of combustion (at 3.6 ms). In such regions the temperature is low and the airflow slows down, which is not conducive to the oxidation of soot. In contrast, the soot of WDEP is mainly generated near the flame axis. The high temperature in the inner region can be maintained for a longer time than that in the outer area. With the combustion process advancing, the soot area moves downward and the local air-fuel ratio gradually increases, creating an environment conducive to soot oxidation. The results above also show that the oxidation of soot in WDEP may be faster, for it is almost completed before the soot is rolled to the edge of the flame by airflow. This is beneficial to reduce residual soot.

With low ambient oxygen concentration, the soot distribution characteristics and soot oxidation are in line with expectations. For WDEP, the soot formation rate is significantly lower because it reduces the over-rich and high temperature region.

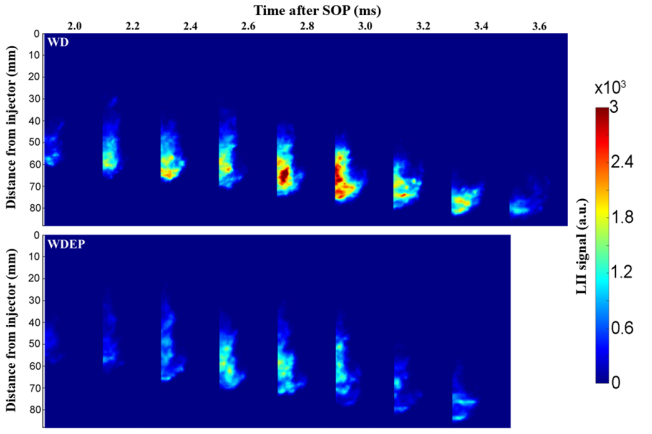

(a) 870 K

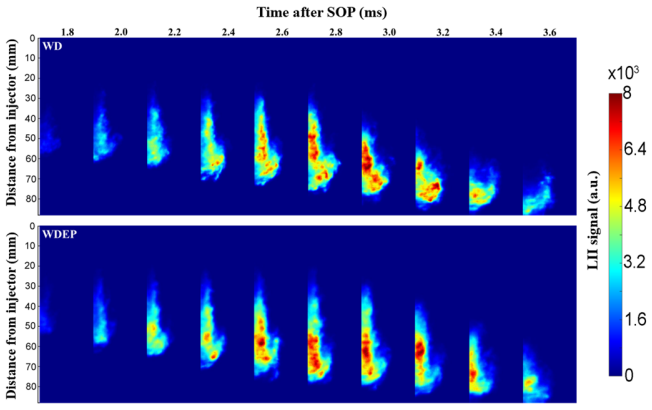

(b) 920 K

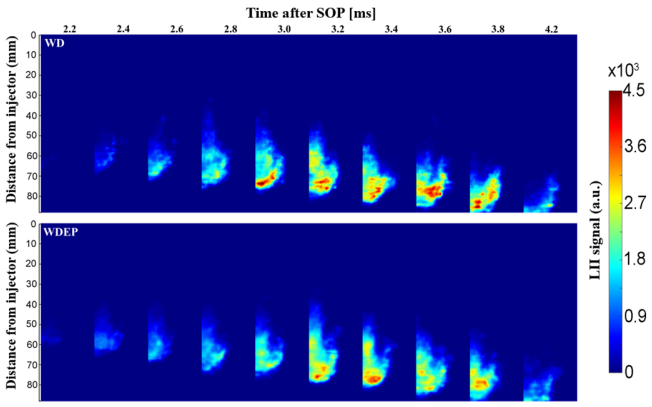

(c) 920 K+EGR

Figure 13. Time sequences of time-varying PLII of WD and WDEP in different ambient conditions.

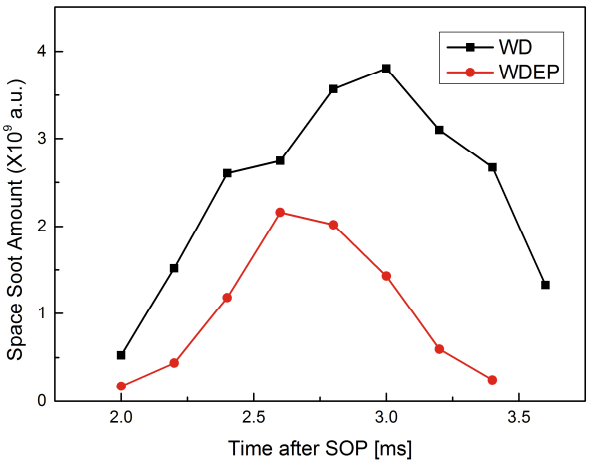

(a) 870 K

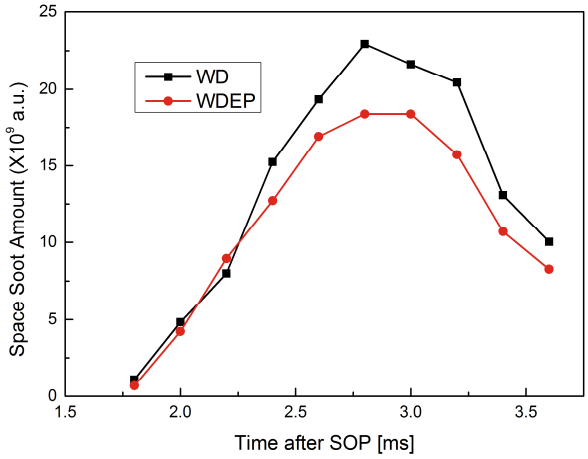

(b) 920 K

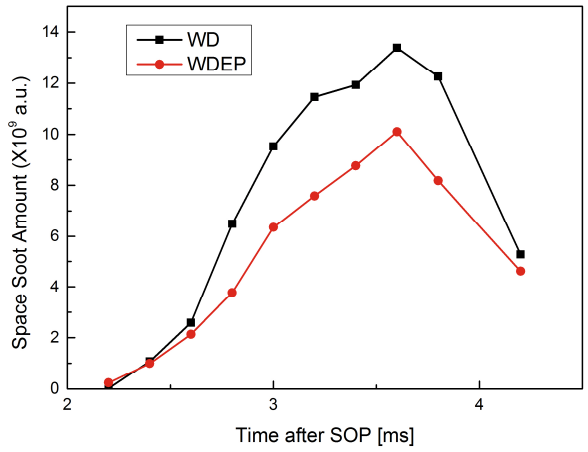

(c) 920 K+EGR

Figure 14. The change trend of space total soot amount with time after injection of tested fuels in different ambient conditions.

Summary/Conclusions

OH * chemiluminescence and PLII were used to study the flame lift-off length, ignition delay and soot distribution of WD, EP and WDEP under different ambient temperature and oxygen concentration. The main conclusions are as follows.

1. The ignition delay and flame lift-off length of WD and WDEP are similar at 870-920 K. The ignition delay of WDEP is less sensitive to ambient oxygen concentration compared with that of WD.
2. For WDEP, the distribution of initial ignition position is more concentrated, especially in the cases with low ambient oxygen concentration.
3. Soot reduction effect of the oxygenated components is more significant at low ambient temperature and low ambient oxygen concentration conditions. Compared with WD, the soot amount of WDEP decreased by 55% and 27% at 870 K and 920 K, for the case of 920 K and 15.8% of ambient oxygen concentration, the soot amount of WDEP decreased by 44%.
4. When EP is added to WD, the distribution area of soot moves inward, the oxidation of soot is accelerated. There is less soot at the edge of flame in the later stage of combustion, which is beneficial to reduce residual soot.

References

1. Kalghatgi, G., Risberg, P., and Ångström, H., "Advantages of Fuels with High Resistance to Auto-ignition in Late-injection, Low-temperature, Compression Ignition Combustion," SAE Technical Paper 2006-01-3385, 2006, doi:10.4271/2006-01-3385.
2. Kalghatgi, G., Risberg, P., and Ångström, H., "Partially Pre-Mixed Auto-Ignition of Gasoline to Attain Low Smoke and Low NOx at High Load in a Compression Ignition Engine and Comparison with a Diesel Fuel," SAE Technical Paper 2007-01-0006, 2007, doi:10.4271/2007-01-0006.
3. Lu, XC., Han, D., Huang, Z., "Fuel design and management for the control of advanced compression-ignition combustion modes," Progress in Energy and Combustion Science 37 (2011) 741-783.
4. Wang, JX., Wang, Z., "Wide distillation fuel and unified internal combustion engines," In: Fundamental science theory and key technology on greenhouse control of internal combustion engine conferenc, Shanghai; 2010.
5. Kalghatgi, G., Johansson B., "Gasoline compression ignition approach to efficient, clean and affordable future engines," J Automobile Engineering, 2018, Vol. 232(1) 118–138
6. Zhang, F., Rezaei, SZ., Xu, HM., Kalghatgi, G., Shuai, SJ., "Combustion and emission characteristics of a PPCI engine fuelled with dieseline," SAE Paper doi:10.4271/2012-01-1138.
7. Weall, A. and Collings, N., "Investigation into Partially Premixed Combustion in a Light-Duty Multi-Cylinder Diesel Engine Fuelled Gasoline and Diesel with a Mixture of gasoline and diesel," SAE Technical Paper 2007-01-4058, 2007, doi:10.4271/2007-01-4058.
8. Zhang, F., Xu, HM., Zhang, J., Tian, G. et al., "Investigation into Light Duty Dieseline Fuelled Partially-Premixed Compression Ignition Engine," SAE Int. J. Engines 4(1):2124-2134, 2011, doi:10.4271/2011-01-1411.
9. Han, D., Ickes, AM., Bohac, SV., Huang, Z., "Assanis DN. Premixed low-temperature combustion of blends of diesel and gasoline in a high speed compression ignition engine," Proc Combust Inst 2011;33:3039-46.
10. Hyun, WW., Pitsch, H., Tai,t N., Kalghatgi, G., "Some effects of gasoline and diesel mixtures on partially premixed combustion and comparison with the practical fuels gasoline and diesel in a compression ignition engine," Proc Inst Mech Eng Part D J Automob Eng 2012;226:1259-70.
11. Yang, HQ., Shuai, SJ., Wang, Z., et al., "High efficiency and low pollutants combustion: gasoline multiple premixed compression ignition (MPCI)," SAE Paper, doi:10.4271/2012-01-0382; 2012.
12. Wang, BY., Shuai, SJ., Yang, HQ, et al., "Experimental study of Multiple Premixed Compression Ignition engine fueled with heavy naphtha for high efficiency and low emissions." SAE Technical Paper, doi:10.4271/2014-01-2678, 2014.
13. Wang, BY., Wang, Z., Shuai, SJ., et al., "Investigations into Multiple Premixed Compression Ignition mode fuelled with different mixtures of gasoline and diesel," SAE Techinal Paper, doi:10.4271/2015-01-0833.
14. Pellegrini, L., Marchionna, M., Patrini, R., Beatrice, C. et al., "Combustion Behaviour and Emission Performance of Neat and Blended Polyoxymethylene Dimethyl Ethers in a Light-Duty Diesel Engine," SAE Technical Paper 2012-01-1053, 2012, doi:10.4271/2012-01-1053.
15. Wang, Z., Liu, HY., Zhang, J., Wang, JX., Shuai SJ., "Performance, combustion and emission characteristics of a diesel engine fueled with polyoxymethylene dimethyl ethers (PODE 3-4)/diesel blends," Energy Procedia; 75:2337-2344, 2015, doi:10.1016/j.egypro.2015.07.479.
16. Ma, X., Ma, Y., Sun, S., Shuai, S. et al., "PLII-LEM and OH* Chemiluminescence Study on Soot Formation in Spray Combustion of $PODE_n$ -Diesel Blend Fuels in a Constant Volume Vessel," SAE Technical Paper 2017-01-2329, 2017, doi:10.4271/2017-01-2329.
17. Liu, H., Wang, Z., and Wang, J., "Performance, Combustion and Emission Characteristics of Polyoxymethylene Dimethyl Ethers (PODE3-4)/ Wide Distillation Fuel (WDF) Blends in Premixed Low Temperature Combustion (LTC)," SAE Int. J. Fuels Lubr. 8(2):2015, doi:10.4271/2015-01-0810.
18. Zheng, L., Ma, X., Wang, Z., Wang, J., "An optical study on liquid-phase penetration, flame lift-off location and soot volume fraction distribution of gasoline–diesel blends in a constant volume vessel," Fuel; 139:365-373, 2015, doi:10.1016/j.fuel.2014.09.009.
19. Schulz, C., Kock, BF., Hofmann, M., et al., "Laser-induced incandescence: recent trends and current questions." Appl Phys B 2006;83(3):333–54.
20. Pickett, LM., Siebers, D., "Soot Formation in Diesel Fuel Jets Near the Lift-Off Length." Int J Engine Res; 7(2):103-130, 2006. doi:10.1243/146808705X57793.
21. Higgins, B., Siebers, D., "Measurement of the flame lift-off location on DI diesel sprays using OH chemiluminescence," SAE Technical Paper 2001-01-0918;2001.
22. Persson, H., Andersson, Ö., and Egnell, R., "Fuel effects on flame lift-off under diesel conditions," Combustion and Flame, 2011. 158(1): p. 91-97.
23. Pickett, LM., Kook, S., Persson, H., Andersson, Ö., "Diesel fuel jet lift-off stabilization in the presence of laser-induced plasma ignition," Proc. Combust. Inst. 32 (2009),2793–2800.

Contact Information

Corresponding author:

Dr. Xiao Ma, Ph. d.
Address: Department of automotive engineering, Tsinghua University, Beijing, 100084, China

max@tsinghua.edu.cn
Phone: +86-10-62772515

Acknowledgments

The present work is sponsored by National Natural Science Foundation of China under Grant 51976100 and 51506111. The authors also acknowledge the support of Chambroad Petrochemicals Co., Ltd, Shandong, China.

Definitions/Abbreviations

EGR	Exhaust gas recirculation
EP	Ethanol- $PODE_n$ blends
LOL	Lift-off length
MPCI	Multiple premixed compression ignition
MPRR	Maximum pressure rise rate
NOx	Nitrogen oxides
PLII	Planar laser induced incandescence
PODE	Polyoxymethylene dimethyl ethers
PPCI	Partial premixed compression ignition
RON	Research octane number
WD	Wide distillation fuel
WDEP	Wide distillation fuel-Ethanol-$PODE_n$ blends